A New FFT Technique for the Analysis of Contact Pressure and Subsurface Stress in a Semi-Infinite Solid

Yong-Joo Cho*
Professor, School of Mechanical Engineering, Pusan National University
Young-Pil Koo, Tae-Wan Kim
Graduate student, Department of Mechanical Engineering, Pusan National University

A numerical procedure for contact analysis and calculating subsurface stress was developed. The procedure takes the advantage of signal processing technique in frequency domain to achieve shorter computing time. Boussinesq's equation was adopted as a response function in contact analysis. The validity of this procedure was proved by comparing the numerical results with the exact solutions. The fastness of this procedure was also compared with other algorithm.

Key Words : Contact Analysis, FFT, Signal Processing, Response Function, Convolution Integral, Boussinesq's Equation, Hertzian Contact, Subsurface Stress

1. Introduction

To analyze tribological phenomena, the contact pressure distribution and subsurface stress field should be evaluated. Nonconforming contacts such as rolling bearing elements or gear teeth are subjected to high contact stresses and the subsurface stresses which cause pitting or spalling. Even in a conformal contact condition, the delamination wear occurred by the cyclic stresses due to the contacts of asperities (Suh, 1977).

Numerous tribological contact problems were studied with Hertzian contact model since his contact analysis (Hertz, 1882) and Greenwood and Williamson (1966) analyzed rough surface contacts with the assumption of spherical shape of asperity tips and Gaussian distribution of asperity heights. A more complicated random process model with spherical asperities was adopted by Bush et. al (1975). The results of their contact models show good estimate on average properties of rough contact in a low contact pressure. However, under the contact of high load, the contacts of adjacent asperities affect each other and those approaches inevitably yield some error.

With the advent of computer, various numerical techniques have been recently developed. Finite element and boundary element methods popular in structural analysis are also used in contact analysis (Anderson, 1982; Webster, 1986; Kwak, 1990). They are powerful in the contact analysis of complex shaped bodies and layered solids. But there are some difficulties in application to 3-dimensional cases. For example, the size of stiffness matrix is very large in 3-dimensional analysis.

The contact area in a tribological problem is relatively small enough to be approximated as the contact on a half space. Most of numerical schemes for the contact analysis in tribology are thus based on Boussinesq's solution. Kalker and Randen (1972) used a numerical technique based on minimum principle of the total internal energy. Tian and Bhushan (1996) calculated the contact of 3-dimensional surfaces with the variational principle. Ren and Lee (1993) adopted the moving grid method to 3-dimensional contact analysis which reduced matrix size in linear equations, saved the computer memory space effectively, and enabled the reduction of calculation time.

* Corresponding Author,
E-mail : yjucho@hyowon. pusan. ac. kr
TEL : +82-51-510-2307 ; **FAX** : +82-51-512-9835
30 Changjeon-Dong, Kum jeong-Gu, Pusan 609-735, Korea. (Manuscript **Received** July 20, 1999 **Revised** December 2, 1999)

But these methods are also inadequate to the analysis of contact of real rough surfaces. To represent the roughness of real surface, a very fine mesh is needed and the number of nodes is increased very much. So most analyses are confined to 2-dimensional(Webster, 1986; Bailey and Sayles, 1991; Komvopoulous, 1992) except a few cases(Tian and Bhushan, 1996; Lai and Cheng 1985).

To overcome this problem, the signal processing technique in frequency domain can be used in the contact analysis. This procedure takes the advantages of Fast Fourier Transformation (FFT). The effectiveness of this procedure is to reduce the computing time substantially in comparison to conventional methods. For example, in the case of the surface with $N \times N$ node numbers, $O(N\log_2 N)$ multiplications are required in the signal process in frequency domain, but in conventional algorithms, the influence matrix of $N^2 \times N^2$ should be constructed and a set of N^2 linear algebraic equations should be solved. Ju and Farris(1996) introduced a FFT method for 2-dimensional line load contact problem. Stanley and Kato(1997) presented the method that took advantages of both FFT and the variational formulation for 2-dimensional and 3-dimensional elastic contact problems of arbitrary topography. Their methods are based on Westergaard's solution of sinusoidal displacement(Westergaard, 1936).

In this study, a new FFT algorithm for the contact analysis is introduced, in which Bouissinesq's equation is used as a response function and subsurface stress is also obtained by FFT algorithm.

2. Analysis Procedure

2.1 Boussinesq's equation

The elastic displacements due to a concentrated point load P at the origin on the surface of a half space are:

$$u_x=\frac{P}{4\pi G}\left\{\frac{xz}{\rho^3}-(1-2\nu)\frac{x}{\rho(\rho+z)}\right\} \quad (1a)$$

$$u_y=\frac{P}{4\pi G}\left\{\frac{yz}{\rho^3}-(1-2\nu)\frac{y}{\rho(\rho+z)}\right\} \quad (1b)$$

$$u_z=\frac{P}{4\pi G}\left\{\frac{z^2}{\rho^3}+\frac{2(1-\nu)}{\rho}\right\} \quad (1c)$$

where $\rho=(x^2+y^2+z^2)^{1/2}$. The surface plane was taken to be the plane z=0, and the positive sense of the axis of z is downwards.

The distributed pressure $p(\xi, \eta)$ acting on the area S produces the displacements in the direction of the load:

$$u_z=\int_S\int\frac{p(\xi,\eta)}{4\pi G}\left\{\frac{z^2}{\rho^3}+\frac{2(1-\nu)}{\rho}\right\}d\xi d\eta \quad (3)$$

where $\rho=\{(x-\xi)^2+(y-\eta)^2+z^2\}^{1/2}$

On the surface of the solid, the displacement is:

$$u_z=\frac{1-\nu}{2\pi G}\int_S\int p(\xi,\ \eta)\cdot h(x-\xi,\ y-\eta)\, d\xi d\eta \quad (4)$$

where $h(\xi, \eta)=\frac{1}{\sqrt{(\xi)^2+(\eta)^2}}$ and displacement u_z due to the distributed pressure p is the convolution of p and h.

2.2 Contact analysis with FFT

With the two functions f_1 and f_2, and their corresponding Fourier transforms $F_1(\omega)$ and $F_2(\omega)$, the Fourier transform of the convolution of the two functions is $F_1(\omega)F_2(\omega)$. The displacement due to the distributed pressure p on the surface, can be expressed in frequency domain as

$$U(\omega_x, \omega_y)=P(\omega_x, \omega_y)H(\omega_x, \omega_y) \quad (5)$$

where $P(\omega_x, \omega_y)$ is the Fourier transform of pressure p and $H(\omega_x, \omega_y)$ is the Fourier transform of h which can be treated as a response function in signal process. Fourier transform of pressure p can be expressed as

$$P(\omega_x, \omega_y)=U(\omega_x, \omega_y)/H(\omega_x, \omega_y) \quad (6)$$

If the surface deformation is known, the contact pressure can be obtained by the inverse Fourier transform of Eq. (5). In conventional techniques, the procedure of getting the contact pressure from the surface deformation is a matrix inversion process or a process of solving a set of linear algebraic equations which are time consuming, but in Eq. (5), that procedure is converted to a simple algebraic procedure of division.

2.3 Subsurface stresses in the solid

Subsurface stresses at a point (x, y, z) are expressed as (LOVE, 1929)

$$\sigma_x=\frac{1}{2\pi}\left(\frac{\lambda}{\lambda+\mu}\frac{\partial V}{\partial z}-\frac{\mu}{\lambda+\mu}\frac{\partial^2\chi}{\partial x^2}-z\frac{\partial^2 V}{\partial x^2}\right) \quad (7a)$$

$$\sigma_y=\frac{1}{2\pi}\left(\frac{\lambda}{\lambda+\mu}\frac{\partial V}{\partial z}-\frac{\mu}{\lambda+\mu}\frac{\partial^2\chi}{\partial y^2}-z\frac{\partial^2 V}{\partial y^2}\right) \quad (7b)$$

$$\sigma_z=\frac{1}{2\pi}\left(\frac{\partial V}{\partial z}-z\frac{\partial^2 V}{\partial z^2}\right) \quad (7c)$$

$$\tau_{yz}=-\frac{1}{2\pi}\left(z\frac{\partial^2 V}{\partial y\partial z}\right) \quad (7d)$$

$$\tau_{zx}=-\frac{1}{2\pi}\left(z\frac{\partial^2 V}{\partial z\partial x}\right) \quad (7e)$$

$$\tau_{xy}=-\frac{1}{2\pi}\left(\frac{\mu}{\lambda+\mu}\frac{\partial^2\chi}{\partial x\partial y}+z\frac{\partial^2 V}{\partial x\partial y}\right) \quad (7f)$$

in which χ is the Boussinesq's 3-d logarithmic potential function, V is the Newtonian potential, λ and μ are Lamé's elastic constants for the material of the solid,

$$\lambda=\frac{E\nu}{(1+\nu)(1-2\nu)},\quad \mu=\frac{E}{2(1+\nu)}$$

When uniform pressure p is applied to the region of the surface consisting of $2a\times 2b$ square, the derivatives of χ and V in stress equation are given in Appendix. By numerical integration of the stresses due to the pressure on the discretized small square over contact area, the subsurface stresses at point (x, y, z) are obtained conventionally. It is a time consuming procedure to calculate the stress distribution in a 3-dimensional body with the numerical double integration of contact pressure by this conventional method. Fortunately, the derivatives of χ and V in stress equation are the functions of $(x-\xi)$ and $(y-\eta)$, thus the stresses due to distributed contact pressure $p(\xi, \eta)$ on the surface S are expressed as convolution integrals. So, the FFT algorithm proposed in Sec. 2.2 is also applicable to calculating the stress distribution in a body caused by contact pressure.

3. Numerical Procedure

Figure 1 is the schematic representation of contact deformation. To solve a contact problem, an iterative procedure is required because of following constraints.

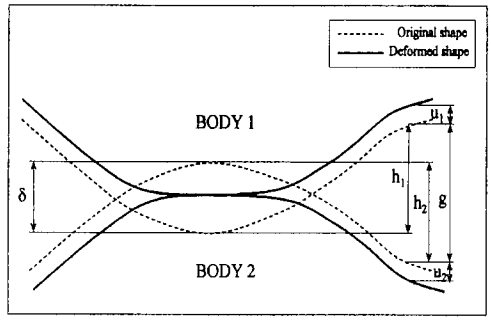

Fig. 1 Schematic representation of the deformation of contact

Inside the contact region:

$$p(x, y)\geq 0,\ g(x, y)=0 \quad (8a)$$

Outside the contact region:

$$p(x, y)=0,\ g(x, y)\geq 0 \quad (8b)$$

where g is the gap between two bodies and p is the contact pressure. g is expressed as

$$g(x, y)=u_1(x, y)+u_2(x, y)+h_1(x, y)+h_2(x, y)-\delta \quad (9)$$

where δ is the relative approach of the two surfaces, $h_1(x)$ and $h_2(x)$ are the height distributions of each surface profile before deformation, and $u_1(x, y)$ and $u_2(x, y)$ are the deformations of each surface. Figure 2 shows the flow diagram for calculating contact pressure and subsurface stress.

4. Numerical Results and Discussion

A new numerical algorithm for contact and subsurface stress distribution was developed.

At first, the contact stress and deformation of the two bodies were solved by FFT method.

The numerical results coincides very well with The major advantage of this method is of reducing CPU time in comparison to any other algorithm. The long CPU time has been a big problem in contact analysis. Hertzian contact of rigid sphere and elastic flat plane was taken as an example to show the efficiency of this FFT technique. The example is like this. The radius of the sphere is 100mm, modules of elasticity of plane is 200Gpa and its Poisson's ratio is 0.3. the relative

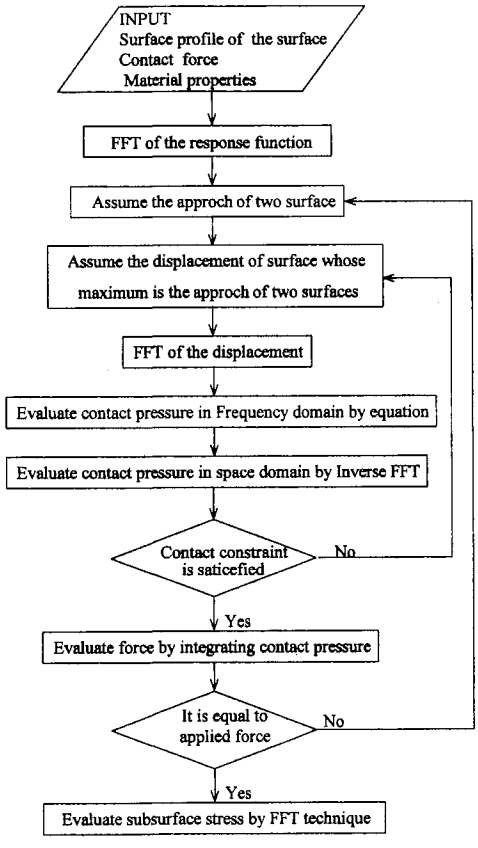

Fig. 2 Flow chart

approach of the two surfaces was set 0.01mm. The number of nodes is 64×64 and grid size is $0.1 \times 0.1\text{mm}^2$. The numerical result was compared with exact solution (Johnson, 1985). Figures 3 and 4 show the contact pressure distribution and displacements in the contact region along x-axis. The numerical result coincides very well with exact solution. Figures 5 and 6 show the three dimensional view of the contact pressures and the deformation of the surface.

In Table 1, the CPU time and accuracy were compared with that of successive over relaxation (SOR) technique which is a most popular numerical procedure in contact analysis. In this case, the number of nodes is 64×64. The CPU time is only about 1/72 of that of SOR technique. As mentioned above, the difference of efficiency depends on the number of nodes. Tian and Bhushan(1996) obtained the solution of Hertzian contact described by 256×256 in 4 days. With the present algorithm, it took less than 30 minutes.

To describe the roughness of a real surface,

Table 1 CPU time and accuracy

Algorithm	SOR method	FFT method	Ratio
CPU time	3600 sec	50 sec	1/72
Error of Maximum Pressure	0.08%	0.07%	

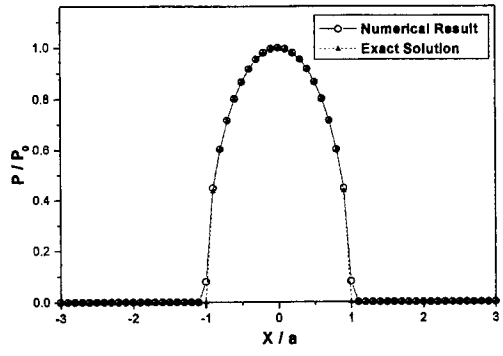

Fig. 3 Contact pressure along x-axis at the surface

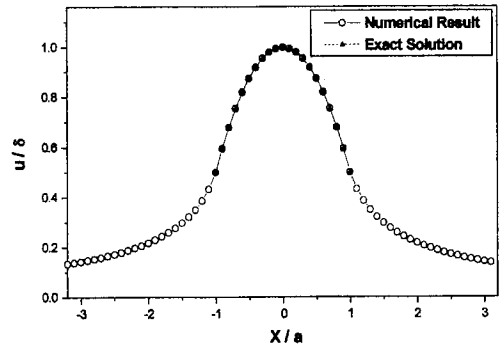

Fig. 4 Displacement along x-axis at the surface

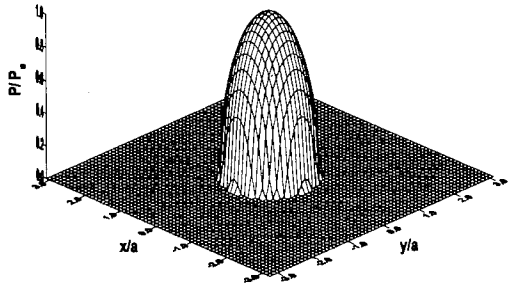

Fig. 5 3-D view of contact pressure in Hetzian contact

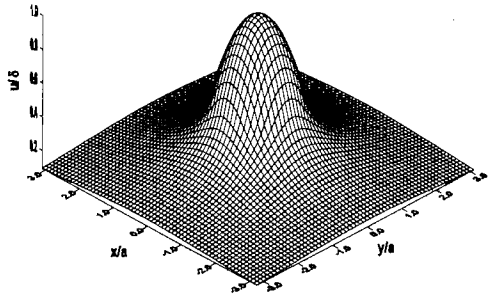

Fig. 6 3-D view of displacement in Hetzian contact

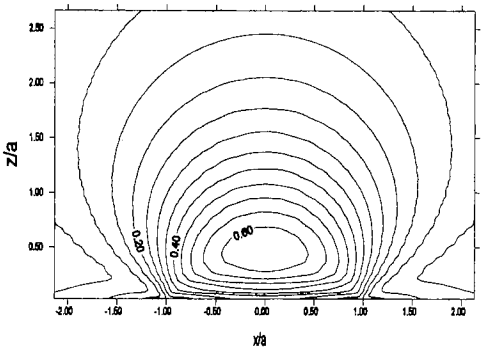

Fig. 7 The equivalent stress distribution on the plane of y=0 in the solid

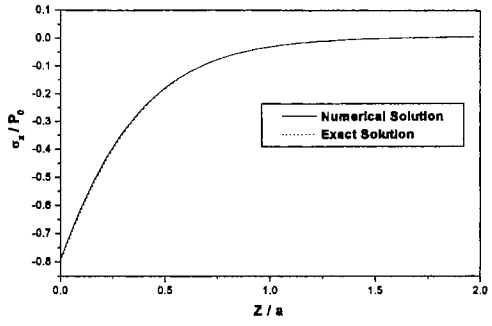

(a) σ_x/p_o along z axis

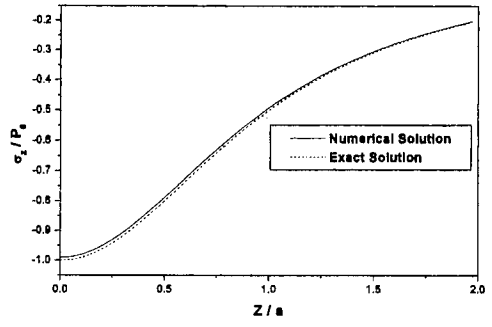

(b) σ_z/p_o along z axis

Fig. 8 Comparison of the numberical results and the exact solution of stress

more nodes may be required. In the analysis of contact of surface which is discretized by $N\times N$ nodes, the influence matrix of $N\times N$ should be constructed and the maximum size of the matrix is radically enlarged to $N^2\times N^2$ in SOR algorithm. As a result, the computing time is exponentially increased with the number of nodes. Considerably long computing time is required with the conventional techniques in analyzing the contact of 3-dimensional rough surfaces.

The same FFT technique is used for calculating the subsurface stresses caused by the above example of Hertzian contact. The stresses were calculated to the depth of 2a. where a is half length of Hertzian contact. The number of nodes along z -axis was 64. The computing time was considerably reduced comparing to conventional numerical integration method. The stresses in Fig. 7 and 8 were normalized by maximum contact pressure p_o. Figure 7 is the equivalent stress distribution on the plane of y=0 in the solid. Maximum equivalent stress is occurred at $0.468a$ and its value is $0.6425p_o$. Their exact solution are $0.464a$ and $0.6434p_o$ respectively.

The numerical results for stress components along z-axis are compared with the exact solution (Johnson, 1985) in Fig. 8.

5. Conclusions

A new numerical technique using FFT was developed for contact analysis and calculating the sub-surface stress, and its efficiency was proved. Boussinesq's equation was adopted as a response function and a filter in frequency domain in this method. The following conclusions are derived from this study.

(1) FFT method was very efficient both in CPU time and in memory size.

(2) FFT method can be effectively used to the calculation of subsurface stress distribution caused by contact pressure.

(3) Numerical results were very well consistent with the exact solution.

Acknowledgement

This research is supported by Korea Science and Engineering Foundations (Contract No. 96-0200-09-01-3). The authors gratefully acknowledge this support.

References

Anderson, T., 1982, "The Second Generation Boundary Element Contact Problem," Boundary elements in Engineering, *Proceedings of Forth International Seminar*, Southampton, England,

Bailey, D. M., and Sayles R. S., 1991, "Effect of Roughness and Sliding Friction on Contact Stresses," *ASME Journal of Tribology*, Vol. 113, pp. 729~738.

Bush, A. W., Gibson, R. D., and Thomas, T. R., 1975, "The Elastic Contact of a Rough Surface," *Wear*, Vol. 35, pp. 87~111

Greenwood, J. A., and Williamson, J. B. P., 1966, "Contact of Nominally Flat Surfaces," *Proceedings of the Royal Society of London*, Vol. A295, pp. 300~319.

Hertz, H., 1882, "Über die Ber hrung fester elastischer Körper," *J. reine und angewandte Mathematik*, Vol. 92, pp. 156~171

Johnson, K. L., 1985, "Contact Mechanics," Cambridge University Press

Ju, Y., and Farris, T. N., 1996, "Spectral Analysis of Two-Dimensional Contact Problems," *ASME Journal of Tribology*, Vol. 118, pp. 320~328.

Kwak, B. M., 1990, "Numerical Implement of Mechanical Engineering," *KSME Iournal*, Vol. 4, No. 1, pp. 23~31

Kalker, J. J., and van Randen, Y., 1972, "A Minimum Principle for Frictionless Elastic Contact with Application to Non-Hertzian Half Space Contact problems," *J. of Eng. Math.*, Vol. 6, pp. 193~206

Komvopoulous, K., and Choi, D. H., 1992, "Elastic Finite Element Analysis of Multi-Asperity Contact," *ASME Journal of Tribology*, Vol. 114, pp. 823~831

Lai, W. T. and Cheng, H. S. 1985, "Computer Simulation of Elastic Rough Contacts," *ASLE Transaction*, Vol. 28, pp. 172~180.

Love, A. E. H., 1929, "The Stress Produced in a Semi-infinite Solid by Pressure on Part of the Boundary," *Phil. Trans. Royal Society*, Vol. A228, pp. 377~420.

Lunderberg, G. and Sj vall, H. 1958, "Stress and Deformation in Elastic Solids," Pub. No. 4 Inst. Th. of Elast., Chalmers University of Technology, Göteborg, Sweden which is referred in "Contact mechanics" by Johnson, K. L., (1985)

Ren, N., and Lee, S. C., 1993, "Contact Simulation of Three-Dimensional Rough Surfaces Using Moving Grid Method," *ASME Journal of Tribology*, Vol. 115, pp. 597~601.

Stanley, H. M., and Kato, T., 1997, "An FFT-Based Method for Rough Surface Contact," *ASME Journal of Tribology*, Vol. 119, pp. 481~485.

Suh, N. P., 1977, "An Overview of the Delamination Theory of Wear," *Wear*, Vol. 44, pp. 1~16.

Tian, X., and Bhushan, B., 1996, "A Numerical Three-Dimensional Model for the Contact of Rough Surfaces by Variational Principle," *ASME Journal of Tribology*, Vol. 118, pp. 33~42.

Webster, M. N., and Sayles, R. S., 1986, "A Numerical Model for the Elastic Frictionless Contact of Real Surfaces," *ASME Journal of Tribology*, Vol. 108, pp. 314~320

Westergaard, H. M., 1939, "Bearing Pressures and Cracks," *ASME Journal of Applied Mechanics*, Vol. 6, pp. A49~A53.

Appendix

The derivatives of potential function χ and V are:

$$\frac{\partial^2\chi}{\partial x^2}=p\Big\{\tan^{-1}\frac{b-y'}{a-x'}+\tan^{-1}\frac{b+y'}{a-x'}-\tan^{-1}\frac{z(b-y')}{(a-x')a_1}$$
$$-\tan^{-1}\frac{z(b+y')}{(a-x')d_4}+\tan^{-1}\frac{b-y'}{a+x'}+\tan^{-1}\frac{b+y'}{a+x'}-\tan^{-1}\frac{z(b-y')}{(a+x')b_2}-\tan^{-1}\frac{z(b+y')}{(a+x')c_3}\Big\}$$

$$\frac{\partial^2\chi}{\partial y^2}=p\Big\{\tan^{-1}\frac{a-x'}{b-y'}+\tan^{-1}\frac{a+x'}{b-y'}-\tan^{-1}\frac{z(a-x')}{(b-y')a_1}$$
$$-\tan^{-1}\frac{z(a+x')}{(b-y')b_2}+\tan^{-1}\frac{a-x'}{b+y'}+\tan^{-1}\frac{a+x'}{b+y'}-\tan^{-1}\frac{z(a-x')}{(b+y')d_4}-\tan^{-1}\frac{z(a+x')}{(b+y')c_3}\Big\}$$

$$\frac{\partial^2\chi}{\partial x'\partial y'}=p\log\frac{(z+a_1)(z+c_3)}{(z+b_2)(z+d_4)}$$

$$\frac{\partial V}{\partial z}=-p\Big\{2\pi-\cos^{-1}\frac{(a-x')(b-y')}{\sqrt{(a-x')^2+z^2}\sqrt{(b-y')^2+z^2}}-\cos^{-1}\frac{(a-x')(b+y')}{\sqrt{(a-x')^2+z^2}\sqrt{(b+y')^2+z^2}}$$
$$-\cos^{-1}\frac{(a+x')(b-y')}{\sqrt{(a+x')^2+z^2}\sqrt{(b-y)^2+z^2}}-\cos^{-1}\frac{(a+x')(b+y')}{\sqrt{(a+x')^2+z^2}\sqrt{(b+y')^2+z^2}}\Big\}$$

$$\frac{\partial^2 V}{\partial x^2}=-p\Big\{\frac{a-x'}{(a-x')^2+z^2}\Big(\frac{b-y'}{a_1}+\frac{b+y'}{d_4}\Big)+\frac{a+x'}{(a+x')^2+z^2}\Big(\frac{b-y'}{b_2}+\frac{b+y'}{c_3}\Big)\Big\}$$

$$\frac{\partial^2 V}{\partial y'^2}=-p\Big\{\frac{b-y'}{(b-y')^2+z^2}\Big(\frac{a-x'}{a_1}+\frac{a+x'}{b_2}\Big)+\frac{b+y'}{(b+y')^2+z^2}\Big(\frac{a-x'}{d_4}+\frac{a+x'}{c_3}\Big)\Big\}$$

$$\frac{\partial^2 V}{\partial z^2}=p\Big\{\frac{a-x'}{(a-x')^2+z^2}\Big(\frac{b-y'}{a_1}+\frac{b+y'}{d_4}\Big)+\frac{a+x'}{(a+x')^2+z^2}\Big(\frac{b-y'}{b_2}+\frac{b+y'}{c_3}\Big)$$
$$+\frac{b-y'}{(b-y')^2+z^2}\Big(\frac{a-x'}{a_1}+\frac{a+x'}{b_2}\Big)+\frac{b+y'}{(b+y')^2+z^2}\Big(\frac{a-x'}{d_4}+\frac{a+x'}{c_3}\Big)\Big\}$$

$$\frac{\partial^2 V}{\partial x\partial z}=p\Big\{\frac{z}{(a-x')^2+z^2}\Big(\frac{b-y'}{a_1}+\frac{b+y'}{d_4}\Big)-\frac{z}{(a+x')^2+z^2}\Big(\frac{b-y'}{b_2}+\frac{b+y'}{c_3}\Big)\Big\}$$

$$\frac{\partial^2 V}{\partial x\partial z}=p\Big\{\frac{z}{(b-y')^2+z^2}\Big(\frac{a-x'}{a_1}+\frac{a+x'}{b_2}\Big)-\frac{z}{(b+y')^2+z^2}\Big(\frac{a-x'}{d_4}+\frac{a+x'}{c_3}\Big)\Big\}$$

$$\frac{\partial^2 V}{\partial x\partial y}=p\Big(\frac{1}{a_1}-\frac{1}{b_2}+\frac{1}{c_3}-\frac{1}{d_4}\Big)$$

where a_1, b_2, c_3, d_4 are the distances of a point of (x, y, z) from corners of the pressed surface square whose center is at $(\xi, \eta, 0)$ and x', y' are $x-\xi$, $y-\eta$ respectively